Journal of Power Sources 234 (2013) 82–90

Contents lists available at SciVerse ScienceDirect

Journal of Power Sources

journal homepage: www.elsevier.com/locate/jpowsour

Electrochemical Ostwald ripening of Pt and Ag catalysts supported on carbon

Preethy Parthasarathy, Anil V. Virkar*

Department of Materials Science and Engineering, 122 S. Central Campus Drive, University of Utah, Salt Lake City, UT 84112, USA

HIGHLIGHTS

- Investigated electrochemical coarsening in Pt and Ag commercial catalysts.
- Developed a method to study electrochemical coarsening of catalysts.
- Studied the effect of electrolyte ion concentration in coarsening kinetics of Pt and Ag.
- The higher the ion concentration, the faster the coarsening kinetics.
- The lower the Pt^{2+} ion concentration in PEMFC electrodes, the greater the stability.

ARTICLE INFO

Article history:
Received 17 November 2012
Received in revised form
15 January 2013
Accepted 18 January 2013
Available online 28 January 2013

Keywords:
Catalysts
PEMFC
Electrochemical coarsening
Coupled transport

ABSTRACT

Electrochemical Ostwald ripening in Pt and Ag commercial catalysts supported on high surface area carbon is investigated by an electrochemical method. The procedure consists of immersing two graphite rods – one with nano Pt or Ag painted on it and the other with bulk Pt or Ag wire wrapped around it – in an electrolyte solution containing Pt or Ag ions. The chemical potential of nano Pt or Ag is expected to be higher than the chemical potential of bulk Pt or Ag due to the Gibbs–Thompson effect. Thus, nano Pt or Ag electrode becomes electrically negative, consistent with its higher chemical potential. The voltage measured decreases with time as the nanoparticles coarsen and the difference in chemical potentials between the two electrodes decreases. The coarsening process involves coupled transport of Pt or Ag ions through the electrolyte and of electrons through the carbon/graphite support. The effect of electrolyte composition on nanoparticles coarsening is also investigated. Despite high Pt^{4+} concentration in the electrolyte, coarsening of Pt is relatively slow due to low Pt^{2+} concentration in the electrolyte.

1. Introduction

Proton exchange membrane fuel cells (PEMFCs) are electrochemical devices which have applications in areas such as transportation, distributed power and portable power. While considerable progress has been made over the past two decades on the PEMFC, it is well known that degradation in performance occurs over time. There are many factors which influence PEMFC degradation. One of the main factors is the degradation (coarsening) of the catalyst on the cathode side. Typically, both the cathode and the anode of a PEMFC contain nanosize noble metal (Pt) or noble metal alloy particles supported on high surface area (HAS) carbon [1–8].

Several mechanisms of cathode degradation have been reported [9–20]. They include: (a) Detachment of catalyst particles from carbon support thus rendering them electro-catalytically inactive. One of the primary reasons for catalyst particle detachment is the oxidation of the supporting high surface area (HAS) carbon. (b) Ostwald ripening of particles. (c) Agglomeration and associated growth (sintering) of particles. (d) Dissolution of the catalyst at the cathode, and its transport and precipitation into the membrane. Ostwald ripening, agglomeration and sintering, and precipitation in the membrane all depend upon some aspects of local dissolution of Pt, its transport, and its precipitation. The thermodynamic driving force for agglomeration/sintering and Ostwald ripening is the reduction in surface energy accompanying particle growth. This phenomenon leads to dissolution of smaller particles and growth of larger particles. In the PEMFC, transport of electrically neutral Pt occurs via a coupled process involving the transport of ions (Pt^{2+} and/or Pt^{4+}) through an ionomer/aqueous medium and a parallel (coupled) transport of electrons through the carbon support, a process which can be termed 'electrochemical coarsening' or 'electrochemical Ostwald ripening' [21]. The importance of parallel electron transport in electrochemical coarsening was also

* Corresponding author. Tel.: +1 801 581 5396; fax: +1 801 581 4816.
E-mail addresses: anil.virkar@m.cc.utah.edu, anil.virkar@utah.edu (A.V. Virkar).

0378-7753/$ – see front matter © 2013 Elsevier B.V. All rights reserved.
http://dx.doi.org/10.1016/j.jpowsour.2013.01.115

demonstrated experimentally by conducting similar experiments on n-Pt-catalysts supported on alumina, which exhibited no particle growth as alumina is electrically insulating [21]. Yu et al. [22] investigated the coarsening mechanisms of nanoparticles using in situ small angle X-ray scattering (SAXS) technique. Their experimental results and modeling also show that coarsening of n-Pt catalyst occurs primarily due to electrochemical Ostwald ripening.

Fig. 1(a) shows two isolated Pt particles immersed in a Pt ion conducting medium. There is a tendency for Pt ions in the smaller Pt particle to dissolve and precipitate on the larger Pt particle due to the difference in chemical potentials. Since the electron concentration in the solution is negligible, the Pt ion transport shuts down and a quasi-equilibrium is attained. The result is that the smaller particle becomes negatively charged and the larger particle becomes positively charged. Fig. 1(b) shows two isolated Pt particles supported on an electronically conducting material such as carbon used in PEMFC electrodes. In this scenario, Pt ions are transported through the medium and electrons are transported through carbon. Since there is a path for the transport of electrons, a quasi-equilibrium is not established, and electrochemical Ostwald ripening continues to occur. In agglomeration/sintering (Fig. 1(c)) a similar process occurs, in which ion transport occurs through ionomer/aqueous medium and electron transport occurs through a direct particle-to-particle contact. In both (b) and (c), net transport of Pt occurs from the smaller particle to the larger particle by a coupled transport. The above features of electrochemical coarsening can be mechanistically described as follows.

The driving force for coarsening of catalyst is the difference (gradient) in chemical potentials between the larger and the smaller particles. The general expression for the chemical potential of Pt or Ag is given in Ref. [23]

$$\mu_{\mathrm{Pt/Ag}} = \mu^{\mathrm{o}}_{\mathrm{Pt/Ag}} + RT \ln a_{\mathrm{Pt/Ag}} + pV_{m-(\mathrm{Pt/Ag})} \tag{1}$$

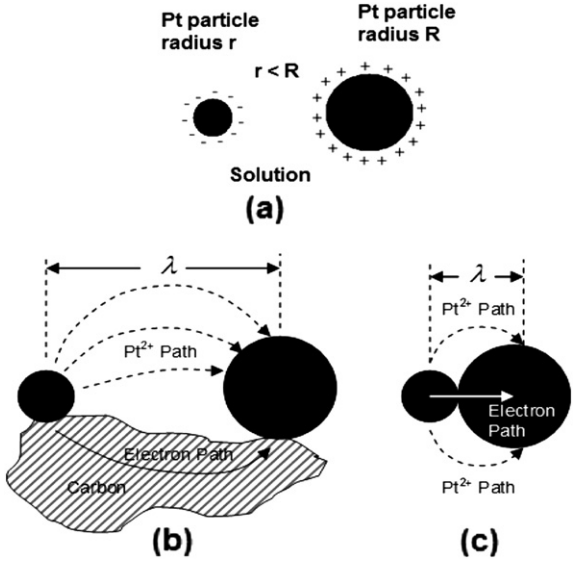

Fig. 1. Mechanism of particle growth by electrochemical Ostwald ripening or agglomeration: (a) two isolated Pt particles dispersed in solution: since no electron path is available, the smaller particle becomes negatively charged and the larger particle becomes positively charged, (b) two isolated particles sitting on carbon support: electrochemical Ostwald ripening – ions transport through the ionomer or aqueous medium and electrons transport through the carbon support, (c) two particles in direct contact with each other: agglomeration/sintering – ions transport through ionomer/aqueous medium and electrons transport through a direct particle-to-particle contact.

where $\mu^{\mathrm{o}}_{\mathrm{Pt/Ag}}$ is the standard state chemical potential of Pt or Ag, $a_{\mathrm{Pt/Ag}}$ is the thermodynamic activity of Pt or Ag, $V_{m-\mathrm{Pt/Ag}}$ is the partial molar volume of Pt of Ag, and p is the pressure. If the material is pure Pt or Ag, then $a_{\mathrm{Pt/Ag}}$ is unity. For a spherical particle of radius r, the pressure created due to the Gibbs–Thompson effect is given by $2\gamma/r$ where γ is the surface energy of the solid/liquid interface. The chemical potential of a particle of Pt or Ag of radius r is therefore given by

$$\mu_{\mathrm{Pt/Ag}} = \mu^{\mathrm{o}}_{\mathrm{Pt/Ag}} + \frac{2\gamma_{\mathrm{Pt/Ag}}}{r} V_{m-(\mathrm{Pt/Ag})} \tag{2}$$

Thus, the smaller the particle size, the higher is the pressure inside the particle, the higher is the chemical potential, and the greater is the tendency for its dissolution and deposition on larger particles. Consider electrochemical coarsening of platinum catalysts. We first consider a schematic of two isolated platinum particles with radii r and R ($r < R$) in a Pt^{2+} ion conducting solution shown in Fig. 1(a). The electrochemical potential of Pt^{2+} ions in a particle radius r is given by,

$$\tilde{\mu}_{\mathrm{Pt}^{2+}}(r) = \mu^{\mathrm{o}}_{\mathrm{Pt}} + \frac{2\gamma V_{m-\mathrm{Pt}}}{r} + 2F\varphi_1 \tag{3}$$

where φ_1 is the electrical potential at the particle of radius r and F is the Faraday constant. The electrical potential φ is given by

$$\varphi = -\frac{\tilde{\mu}_{\mathrm{e}}}{F} = -\frac{\mu_e}{F} + \Phi \tag{4}$$

where μ_{e} is the Fermi energy of Pt and Φ is the electrostatic potential. A quasi-equilibrium is established once the electrochemical potential of Pt^{2+} ions in both particles is the same (equilibrated). That is,

$$\tilde{\mu}_{\mathrm{Pt}^{2+}}(r) = \tilde{\mu}_{\mathrm{Pt}^{2+}}(R) \tag{5}$$

Substituting equation (3) into (5) gives

$$\mu^{\mathrm{o}}_{\mathrm{Pt}} + \frac{2\gamma V_{m-\mathrm{Pt}}}{r} + 2F\varphi_1 = \mu^{\mathrm{o}}_{\mathrm{Pt}} + \frac{2\gamma V_{m-\mathrm{Pt}}}{R} + 2F\varphi_2 \tag{6}$$

where φ_2 is the electric potential at the particle of radius R. Therefore, the electrical potential difference between the two platinum particles of radii r and R is given by,

$$\Delta\varphi = \varphi_1 - \varphi_2 = \left(\frac{\gamma V_{m-\mathrm{Pt}}}{rF} - \frac{\gamma V_{m-\mathrm{Pt}}}{RF}\right) = \frac{\gamma V_{m-\mathrm{Pt}}}{F}\left(\frac{1}{r} - \frac{1}{R}\right) \tag{7}$$

If $R \gg r$, the particle of radius R can be considered as bulk Pt. This gives the electrical potential difference between the particles as

$$\Delta\varphi(r) = \frac{\gamma V_{m-\mathrm{Pt}}}{Fr} \tag{8}$$

The preceding suggests that if one measures the electrical potential difference between a nanosize Pt particle of radius r and the corresponding bulk sample, both immersed in a Pt^{2+} ion conducting medium, one can estimate the size of the nano-particle from the measurement of electric potential difference between the nano and the bulk particles. It also suggests an electrochemical technique to study the electrochemical coarsening of catalysts ex-situ. Fig. 2 shows a schematic of the electrochemical technique developed. In this experiment, one of the graphite rods is painted with nano Pt or Ag catalyst and the other is wound with a bulk Pt or Ag wire. The former serves as an n-Pt or n-Ag electrode and the latter as bulk Pt or Ag electrode (with graphite being an inert

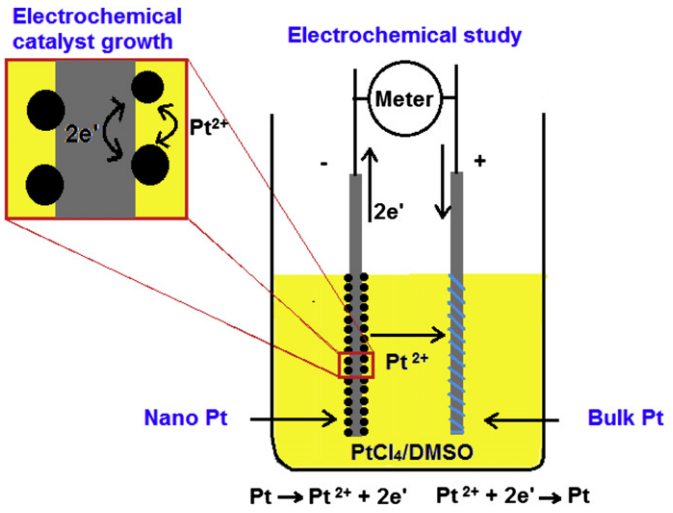

Fig. 2. A schematic of the experimental setup used with n-Pt or/n-Ag as one electrode and bulk Pt or Ag as the other. Inset shows electrochemical catalyst growth occurring on the nanoelectrode which leads to the coarsening of the nanoparticles in the electrode.

material). Both electrodes are immersed in a Pt or Ag ion solution with negligible electronic conduction. This is similar to the process described in Fig. 1(a). Once quasi-equilibrium is attained, the electrochemical potential of Pt or Ag ions is equilibrated on both the electrodes. The potential difference measured between the two electrodes depends on the average particle size of the nano-electrode and provides a direct measure of the average particle size in the n-Pt or n-Ag electrode. The inset in Fig. 2 shows the electrochemical coarsening process that occurs at the nanoelectrode while immersed in the solution. This process is the same as described in Fig. 1(b) in which the two particles are supported on a carbon support. In this case, a quasi equilibrium is not attained between the two particles as the carbon support is an excellent conductor of electrons, and continuous transport of Pt or Ag occurs by a coupled process from the smaller particle to the larger particle. That is, Pt or Ag ions continue to be transported from the smaller particles to the larger particles and the corresponding electrons are transported through the carbon support. As particle growth occurs, the average particle size in the n-Pt (n-Ag) electrode increases, which reflects as a decrease in the voltage measured between the n-electrode and the bulk-electrode. This paper investigates the degradation kinetics of commercial Pt or Ag catalysts supported on high surface area (HAS) carbon ex-situ by conducting experiments in Pt or Ag salt solutions.

2. Experimental procedure

2.1. Electrochemical studies on n-Pt commercial catalyst supported on carbon

In one experiment, n-Pt catalyst supported on high surface area (HAS) carbon (E-TEK) (Somerset, NJ) was immersed in 0.1 M $PtCl_4$ solution in dimethyl sulfoxide (DMSO) at room temperature. Powder samples were removed from the solution after 1 day, 3 days, 5 days, and 7 days. The samples were washed, dried and examined under a transmission electron microscope (TEM). In the other set of experiments, the experimental arrangement shown in Fig. 2 was used. Pt wire of 127 μm diameter, wrapped on a graphite rod, was used as the bulk Pt (counter) electrode. n-Pt catalyst supported on high surface area (HAS) carbon, painted on another graphite rod, served as the n-Pt (working) electrode. The two rods were partially immersed in a Pt-salt solution in DMSO. Any voltage created between the rods (electrodes) was measured using an electrometer (Keithley 6514) with a high input impedance (>200 Tera Ω). The effects of various parameters on the kinetics of coarsening were investigated: (a) The effect of the concentration of $PtCl_4$ in $PtCl_4$ + DMSO solution: Experiments were conducted using 0.001 M $PtCl_4$ + DMSO, 0.01 M $PtCl_4$ + DMSO, and 0.1 M $PtCl_4$ + DMSO electrolyte solutions. (b) The effect of the valence of the Pt-ion: Experiments were conducted using 0.01 M $PtCl_4$ + DMSO and 0.01 M $PtCl_2$ + DMSO solutions as the electrolytes. Samples were examined under a TEM. The particle size distributions were calculated from the TEM micrographs of the samples.

2.2. Electrochemical studies on n-Ag commercial catalyst supported on carbon

Similar experiments using the setup shown in Fig. 2 were conducted to investigate electrochemical coarsening of n-Ag. One of the graphite rods was wrapped with silver wire of 200 μm diameter which served as the bulk silver electrode. The other graphite rod was painted with a silver paste made of silver nanoparticles supported on high surface area carbon (BASF) (Iselin, NJ). The two graphite rods were partially immersed in various concentrations of silver salt solutions in DMSO: 0.1 M $AgNO_3$ + DMSO, 0.001 M $AgNO_3$ + DMSO and 36 μM AgCl + DMSO. The experiment in each case was conducted for about 5–10 min. The time dependence of voltage decay was recorded and was analyzed to investigate the kinetics of electrochemical coarsening. The kinetics of coarsening of silver nanoparticles was also studied by analyzing the samples using TEM and the corresponding particle size distributions were calculated.

3. Results and discussion

3.1. Experimental results and calculations on particle growth from TEM observations and the electrochemical technique

Fig. 3(a–d) shows transmission electron micrographs (TEM) of platinum nanoparticles supported on high surface area (HAS) carbon treated under different conditions. Fig. 3(a) shows a TEM image of the as-received Pt catalyst supported on carbon (E-TEK). The average Pt particle size (diameter) is 2.1 ± 1.4 nm. Fig. 3(b–d) respectively shows TEM images of the Pt catalyst after 1 day, 5 days and 7 days in 0.1 M $PtCl_4$ + DMSO. The corresponding average particle sizes were respectively, 4.0 ± 1.9 nm, 8.5 ± 7.9 nm and 11.3 ± 8.2 nm. After ∼1 week in the electrolyte solution, the Pt particles coarsened to about six times the initial particle size.

In order to ensure that the voltage measured between the two electrodes using the electrochemical technique (Fig. 2) is representative of the actual difference in the chemical potentials between the bulk and the nanoelectrodes, an experiment was conducted using the experimental arrangement shown in Fig. 2 in which both electrodes were identical. In this experiment, n-Pt catalyst supported on high surface area carbon (E-TEK) was painted on both graphite electrodes. Fig. 4 shows the measured voltage between the two identical electrodes when immersed in 0.1 M $PtCl_4$ + DMSO solution. Note that the voltage between the two identical n-Pt electrodes attained ∼0 V after an initial transient. Since identical reactions are expected to occur at the two electrodes and they are connected in series in opposite directions, electrode reactions that occur at one electrode are mirrored in the other electrode thereby canceling the effects. Such is not the case when the two electrodes are different, one nano and the other bulk. Thus, the measured voltage between the n-Pt electrode and the bulk Pt

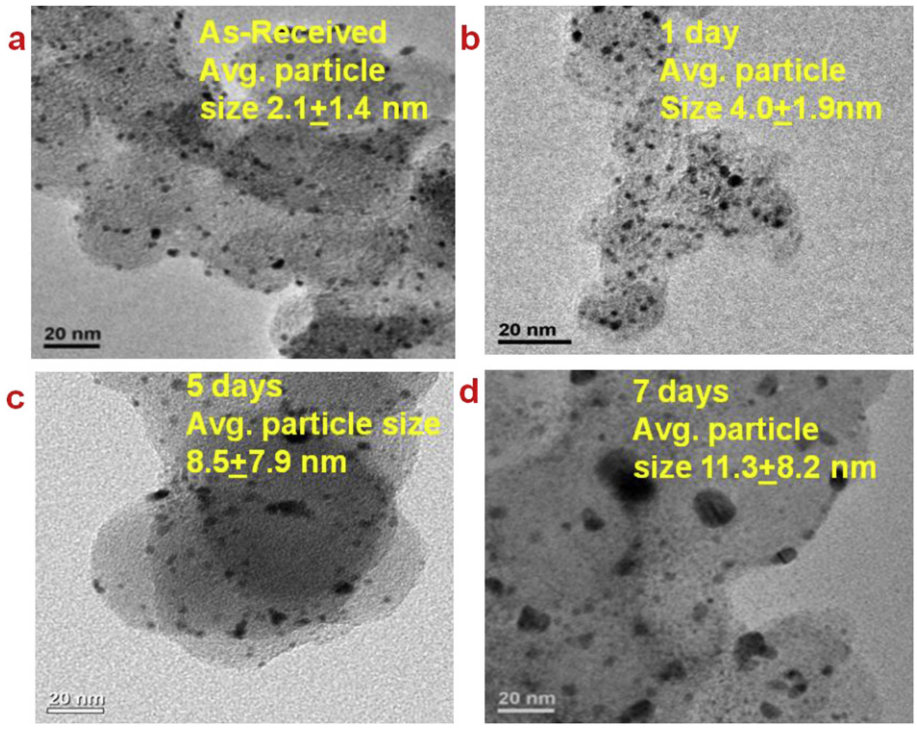

Fig. 3. (a) As-received Pt catalyst supported on carbon (E-TEK). Pt catalyst in 0.1 M $PtCl_4$ in DMSO: (b) after 1 day, (c) 5 days, (d) 7 days.

electrode (Fig. 2) as a function of time can be attributed to the coarsening of platinum nanoparticles by a coupled transport of Pt ions and electrons when submerged in the electrolyte.

Fig. 5 shows the voltage vs. time plot for the experiment conducted using n-Pt and bulk Pt on graphite rods as the electrodes (Fig. 2) in 0.1 M $PtCl_4$ + DMSO solution as the electrolyte. The experiment was conducted for about 7 days. The voltage between the n-Pt electrode and the bulk Pt electrode decreased from the initial ~42 mV to ~8 mV at the end of 7 days. The graphite rod with bulk platinum exhibited a positive potential with respect to the n-Pt electrode. As stated earlier, this is because the chemical potential of Pt in the nanoparticles is higher than that of the bulk Pt, thus rendering a positive charge to the bulk Pt. In the electrochemical Ostwald ripening process, platinum ions transport from the smaller nanoparticles to the larger nanoparticles through the electrolyte while electrons transport through the carbon support/graphite rod. As the nanoparticles coarsen, their chemical potential decreases and the voltage between the bulk Pt-electrode and the n-Pt electrode decreases with time. The average particle size and size distributions were determined on Pt-catalyst supported on carbon immersed in 0.1 M $PtCl_4$ + DMSO solution for various periods of time using the TEM micrographs shown in Fig. 3(a–d). In the literature, the surface energy of platinum in free space is reported to be ~2.23 J m^{-2} [24,25]. In the present work,

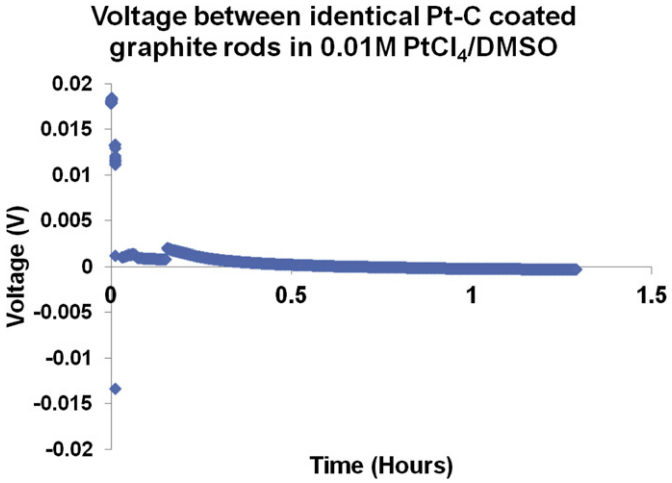

Fig. 4. A voltage vs. time plot of identical electrodes immersed in a 0.1 M $PtCl_4$ + DMSO solution – the electrodes being n-Pt painted on graphite rods. After an initial transient the voltage stabilizes to 0 V.

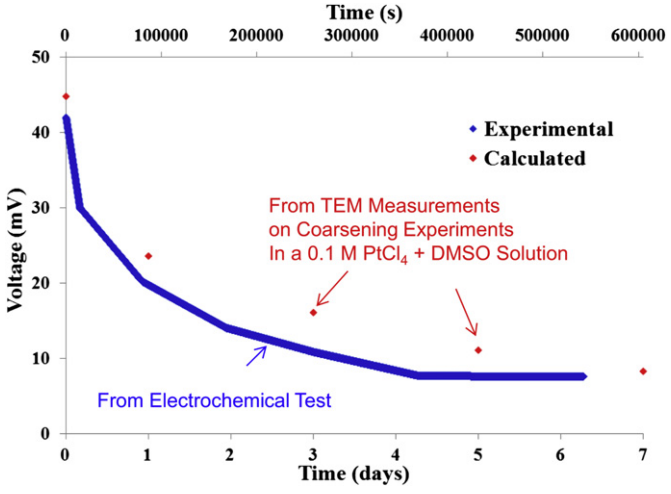

Fig. 5. Voltage vs. time plot of Pt–C catalysts measured with respect to bulk platinum in 0.1 M $PtCl_4$ + DMSO for ~7 days. The datapoints (diamonds) represent the voltage calculated assuming $\gamma = 0.5$ J m^{-2} using the corresponding particle sizes of Pt catalyst treated for various test durations – as-received, 1 day, 3 days, 5 days and 7 days in 0.1 M $PtCl_4$ + DMSO solution. The measured voltage appears segmented instead of a continuous curve due to a temporary issue with the recording software.

since platinum is in contact with an electrolyte, the solid/liquid surface energy of platinum is expected to be lower due to the possible adsorption of other species, e.g. Cl^- ions. We assume γ to be 0.5 J m^{-2}which gives a reasonable agreement with the initial voltage between the nano and the bulk platinum electrodes. The $\Delta\varphi$ was calculated using equation (7) based on the average particle sizes of platinum catalyst determined from the aging experiments and assuming γ to be 0.5 J m^{-2}. The calculated voltage is compared to the experimental values in Fig. 5, which shows very good agreement.

3.2. Coarsening kinetics of n-Pt

Fig. 6 shows the particle size distributions of platinum nanoparticles supported on high surface area carbon (ETEK) treated in 0.1 M $PtCl_4$ + DMSO solution for various durations: 1 day, 3 days, 5 days and 7 days and compared to the as-received platinum catalyst sample (TEM images in Fig. 3(a–d)). For determining each distribution, diameters were manually measured from TEM micrographs with the sampling sizes between 150 and 250 particles for each sample. The measured data were fitted to a normal distribution using the software OriginLab. The growth of particles and the broadening of the distribution are clearly seen in the samples treated for 1 day, 3 days, 5 days and 7 days. The distributions for the samples treated for 5 days and 7 days are considerably broader and have shifted to the right. It is known that in a quasi-steady state, particle size distribution undergoing Ostwald ripening can be described by Lifschitz–Slyozov–Wagner (LSW) distribution [26,27]. By contrast, in agglomeration/sintering, the typical size distribution in a quasi-steady state obeys lognormal distribution. None of these two distributions adequately describes the distributions observed in the present work. This in part suggests that quasi-steady state distributions were probably not established over the durations of the present experiments and the measured distributions thus are representative of transient states. It is for this reason the observed particle size distributions were fitted assuming a normal distribution. The goodness of the fit achieved was poor in each case. This may be due in part to the wide distribution of particle sizes as well as the effect of agglomeration/sintering of particles during coarsening. Also, the sampling size was rather small (less than 250 particles counted for any given sample). Fig. 7 shows a plot of the kinetics of coarsening of platinum nanoparticles for a duration of upto 7 days. Lifshitz–Slyozov [26] and Wagner [27] theory shows that coarsening follows a temporal power law $\overline{d}_t^n \propto t$ with exponent $n = 3$ for a diffusion-controlled process and $n = 2$ for an interface-controlled process, where $\overline{d}_t^n$ is the expectation value of the nth moment of the particle size, provided a quasi-steady state is established. In the present work, coarsening exhibits a linear dependence on time. That is,

$$\overline{d}(t) - \overline{d}(0) = 2\overline{r}(t) - 2\overline{r}(0) = k_L t \quad (9)$$

The rate constant k_L is determined from Fig. 7 as 1.58×10^{-14} m s^{-1} for the platinum catalyst treated in 0.1 M $PtCl_4$ + DMSO solution for 7 days. A previous study by the authors on the kinetics of copper particle coarsening in aqueous media also showed a linear dependence on time [28]. The linear dependence may be due to the presence of agglomeration/sintering during the coarsening process. When agglomeration occurs, two particles are in contact. During coarsening, the center-to-center distance of the two particles decreases which results in a further increase in the driving force. Thus, the kinetics appears to be interface-controlled with the decrease in inter-particle distance between the particles in contact resulting in approximately linear dependence of particle size on time. Also, the observed size distributions could not be fitted to either LSW distribution or lognormal distribution, suggesting that a quasi-steady state, insofar as growth kinetics is concerned, was probably never established over the duration of the present experiments.

3.3. The effect of electrolyte concentration on n-Pt coarsening

Fig. 8 shows voltage vs. time plots for the experiments conducted using n-Pt supported on carbon and bulk platinum on

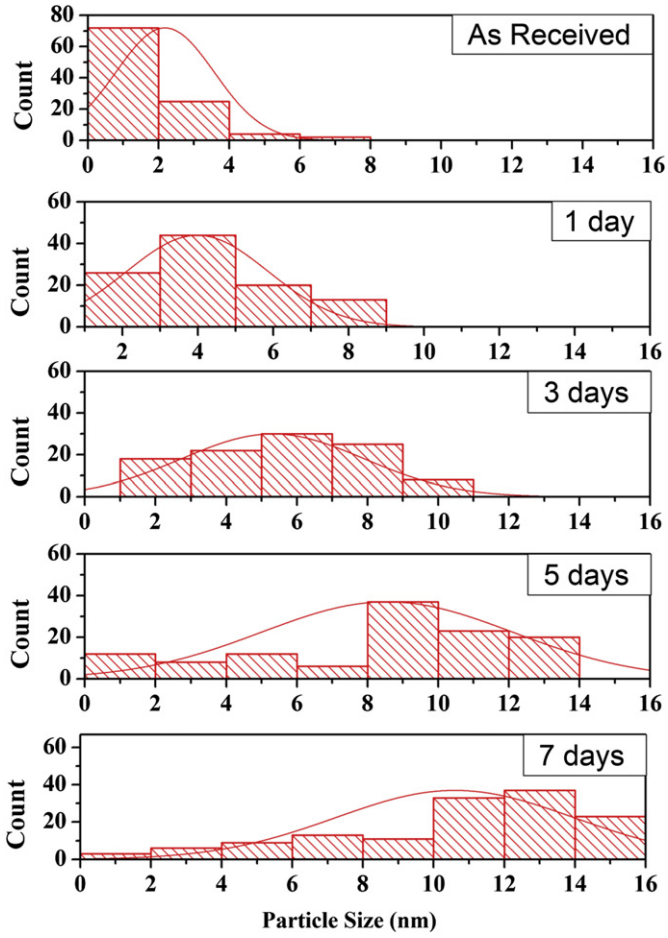

Fig. 6. Particle size distributions of Pt–C (E-TEK) treated in 0.1 M $PtCl_4$ + DMSO electrolyte solution for various durations up to 7 days.

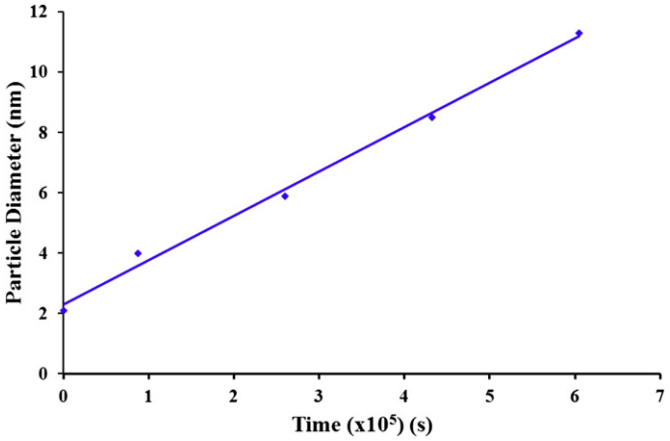

Fig. 7. The kinetics of coarsening of platinum catalyst supported on HAS carbon (E-TEK) treated in a 0.1 M $PtCl_4$ + DMSO solution for various durations upto 7 days. Coarsening exhibits a linear dependence on time.

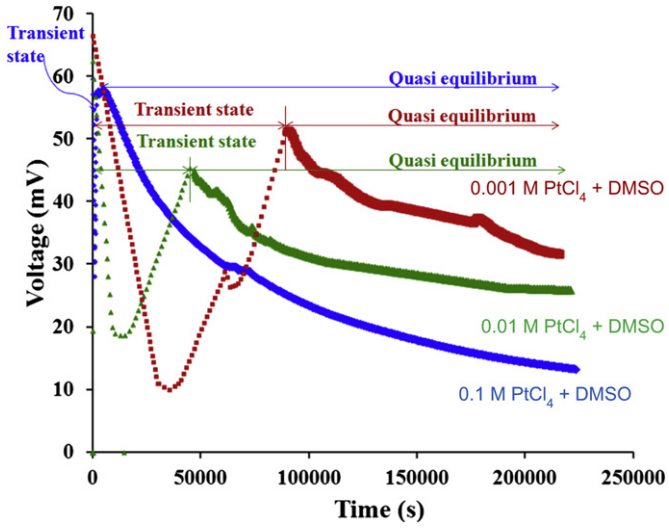

Fig. 8. Voltage vs. time plots for n-Pt–C catalysts supported on HAS carbon measured with respect to bulk platinum in 0.1 M $PtCl_4$ + DMSO, 0.01 M $PtCl_4$ + DMSO and 0.001 M $PtCl_4$ + DMSO solutions as electrolytes for ~60 h.

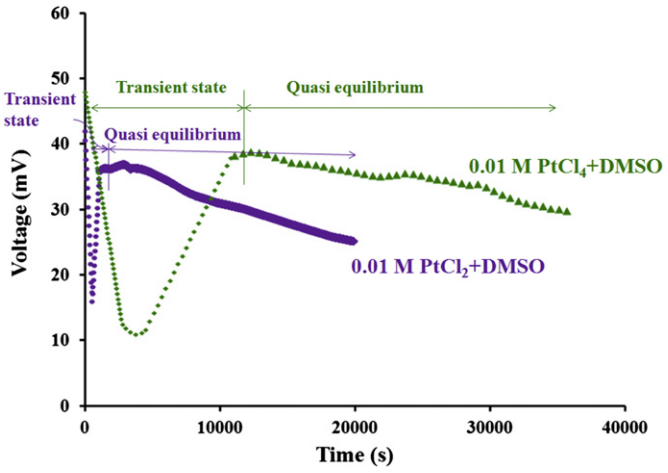

Fig. 9. Voltage vs. time plots of n-Pt catalysts supported on HAS carbon (E-TEK) measured with respect to bulk platinum in 0.1 M $PtCl_4$ + DMSO and 0.1 M $PtCl_2$ + DMSO solutions as electrolytes for ~10 h.

graphite rods as the electrodes in 0.1 M $PtCl_4$ + DMSO, 0.01 M $PtCl_4$ + DMSO and 0.001 M $PtCl_4$ + DMSO solutions as the electrolytes. Each experiment was conducted for ~60 h. These experiments were conducted in order to investigate the effect of Pt ion concentration on the kinetics of coarsening of Pt nanoparticles. The time dependence of the voltage variation with time for the higher concentration electrolyte (0.1 M $PtCl_4$ + DMSO solution) is similar to the voltage variation given in Fig. 5, which is also for 0.1 M $PtCl_4$ + DMSO solution, showing the general reproducibility of the experiments. Fig. 8, however, shows that for the measurements made in more dilute solutions, there is an initial transient stage in which the measured potential initially decreases, and then increases. The decrease in voltage with increasing time in the transient stage probably represents the initial dissolution of Pt ions from the nanoparticles into the solution making the nanoelectrode more negative. The rise in voltage with increasing time (still in the transient regime) is attributed to the transport of Pt ions (assumed to be Pt^{2+}) from the n-Pt to the bulk-Pt electrode. This is expected to occur by diffusion and natural convection. It is expected that at the end of the transient stage, a quasi-equilibrium is established such that the electrochemical potential of Pt^{2+} ions in both n-Pt and bulk-Pt electrodes is nearly identical. The gradual decrease in voltage past the transient stage is attributed to the coarsening of n-Pt. As seen in Fig. 8, the lower the Pt ion concentration in the electrolyte, the longer is the transient stage. This observation is in accord with expectation that transport kinetics should be faster in electrolytes containing higher Pt ion concentration. Also note that the lower the Pt ion concentration, the higher is the measured voltage once quasi-equilibrium is established, indicating slower kinetics of particle growth. Thus, as observed in the plots, it is clear that the lower the concentration of Pt ions in the electrolyte, the slower is the kinetics of coarsening of Pt nanoparticles.

In order to investigate the effect of the valence of Pt in the salt, and the possible effect of Pt^{2+} ion concentration on the kinetics of coarsening, similar experiments were conducted with 0.01 M $PtCl_2$ + DMSO and 0.01 M $PtCl_4$ + DMSO solutions as the electrolytes. Fig. 9 shows the voltage vs. time plots of the above experiments conducted for about 10 h. As seen in Fig. 9, the kinetics of coarsening of Pt nanoparticles supported on HAS carbon treated in 0.01 M $PtCl_2$ + DMSO solution is faster than that in 0.01 M $PtCl_4$ + DMSO solution. Furthermore, quasi-equilibrium was achieved much faster in the experiment with 0.01 M $PtCl_2$ + DMSO as the electrolyte. These observations are consistent with the expectation that the Pt^{2+} concentration in a 0.01 M $PtCl_2$ + DMSO solution will be higher than in 0.01 M $PtCl_4$ + DMSO solution, since in the latter Pt^{2+} ions are formed by the chemical reaction $Pt + PtCl_4 \rightarrow 2PtCl_2$ at the solution/Pt interface. The present results thus suggest that the ions responsible for the coarsening of Pt nanoparticles are Pt^{2+} even though the salt used was $PtCl_4$. In our previous work [29] we investigated the effect of stress on the dissolution/precipitation of platinum using bulk platinum wires/foils. Our study [29] also showed that the dominant electrode reactions involved Pt^{2+} ions even though the electrolyte used was $PtCl_4$ + DMSO solution. Similarly, in the present work, if the transport of Pt^{4+} had been responsible for coarsening, the kinetics would have been much faster than observed in $PtCl_4$ + DMSO electrolytes. This also suggests that there was probably negligible mixed potential effect.

3.4. The effect of electrolyte concentration on n-Ag coarsening

Fig. 10 shows voltage vs. time plots for the experiments conducted using n-Ag supported on carbon (BASF) and bulk Ag on graphite rods as the electrodes with 0.1 M $AgNO_3$ + DMSO, 1 mM $AgNO_3$ + DMSO and 36 μM AgCl + DMSO solutions as the electrolytes. As seen in Fig. 10, the kinetics of voltage decay, a measure of the kinetics of coarsening, is much faster in the case of n-Ag as compared to n-Pt. Note that the experiments on n-Ag were conducted for only 5–10 min (300–600 s). A significant decrease in voltage was observed in all three electrolytes. Even in the electrolyte containing 36 μM AgCl, the voltage decreased sharply. An important observation is that even in 36 μM AgCl solution, the voltage decreased monotonically with time, unlike experiments conducted on n-Pt (Figs. 8 and 9) in which first a sharp drop in voltage followed by an increase was observed. In the case of experiments on n-Ag in AgCl, the solution was saturated with Ag^+ ions since AgCl has very low solubility in DMSO. Thus, dissolution of n-Ag likely does not occur unlike n-Pt in contact with $PtCl_4$ and $PtCl_2$ solutions, which were not saturated. Similar to the n-Pt catalysts, the kinetics of coarsening of n-Ag was faster at higher concentrations of Ag^+ ions present in the solution.

Fig. 11(a–d) shows TEM images of the as-received n-Ag supported catalyst and after the electrochemical coarsening experiments in solutions containing various Ag^+ ion concentrations for

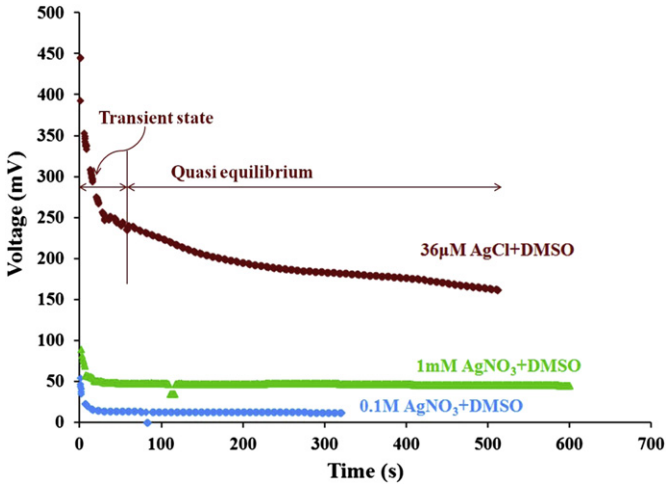

Fig. 10. Voltage vs. time plots of n-Ag catalysts supported on HAS carbon (BASF) measured with respect to bulk silver in 0.1 M $AgNO_3$ + DMSO, 1 mM $AgNO_3$ + DMSO and 36 μM AgCl + DMSO solutions as electrolytes.

10 min. Fig. 11(a) shows a TEM image of the as-received Ag catalyst supported on carbon (BASF). The average Ag particle size (diameter) is 3.9 ± 1.9 nm. Fig. 11(b) shows a TEM image after 600 s in 36 μM AgCl solution in DMSO, with an average particle size of 4.4 ± 3.2 nm. Fig. 11(c) is a TEM image after 600 s in 1 mM $AgNO_3$ solution in DMSO. The average Ag particle size is 6.5 ± 8.7 nm. Finally, Fig. 11(d) is a TEM image after 600 s in 0.1 M $AgNO_3$ solution in DMSO, which has an average size of 8.7 ± 7.7 nm. A large standard deviation is consistent with rather wide distributions. Also, because of the use of normal distribution for fitting, positive values of the probability at negative values of the size are seen in one instance. This is simply because of the choice of the normal distribution made in data fitting.

In AgCl + DMSO, the initial voltage was very high (~445 mV) and decreased to ~163 mV in 10 min. It is possible that quasi-equilibrium was not achieved in this case over the duration of the experiment, possibly due to the very low Ag^+ concentration. Assuming quasi-equilibrium, an estimate of solid/liquid surface energy using $\gamma = r\Delta\varphi(r)F/2V_{m-Ag}$ with $\Delta\varphi(r) = 163$ mV at the end of the test and the measured average particle radius of $r = 2.2$ nm, gives $\gamma \approx 1.68$ J m^{-2}. A similar estimate of solid/liquid surface energy for the sample treated in 1 mM $AgNO_3$ electrolyte solution at the end of the test using $\Delta\varphi(r) = 46$ mV and $r = 3.25$ nm gives $\gamma \approx 0.7$ J m^{-2}. Finally, for the test conducted in 0.1 M $AgNO_3$ solution, with $\Delta\varphi(r) = 12$ mV and $r = 4.35$ nm gives $\gamma \approx 0.25$ J m^{-2}. The reported solid-vacuum surface energy for silver is about 1.2 J m^{-2} [30]. The estimated values of solid/liquid surface energies in $AgNO_3$ solutions of 0.7 J m^{-2} in 1 mM and 0.25 J m^{-2} in 0.1 M may be reasonable given that higher concentrations of adsorbed species would be expected in solutions with higher salt concentrations, thus lowering the surface energy. In AgCl solution with salt concentration in the μM range, the estimated higher surface energy

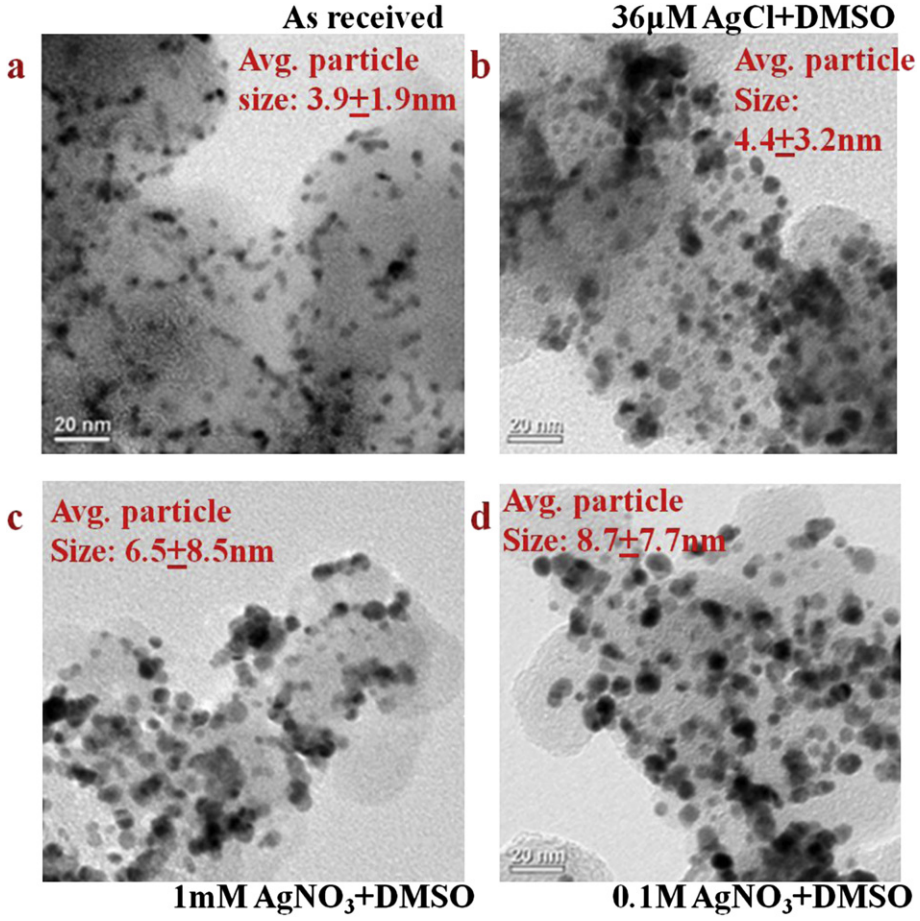

Fig. 11. (a) TEM image of the as-received Ag catalyst supported on HAS carbon (BASF). TEM images of the catalyst after 600 s in: (b) 36 μM AgCl + DMSO, (c) 1 mM $AgNO_3$ + DMSO, (d) 0.1 M $AgNO_3$ + DMSO solutions.

appears to be consistent with low concentration of any adsorbed species.

Fig. 12 compares the particle size distributions of n-Ag treated in electrolytes of various concentrations of $AgNO_3$, namely; 36 μM AgCl + DMSO, 0.1 M $AgNO_3$ + DMSO, and 1 mM $AgNO_3$ + DMSO solutions with the as-received Ag catalyst sample. The average particle size (and size distribution) of the sample treated in 36 μM AgCl + DMSO solution for 500 s is only slightly larger (broader) than that of the as-received Ag sample. This observation is consistent with the relatively high voltage (163 mV) measured at the end of the test. By contrast, in the samples treated in 1 mM and 0.1 M solutions, the average particle size is considerably larger than the initial size, and the distributions are also much broader.

3.5. Implications concerning catalyst degradation in PEMFC

In the present work all experiments were conducted ex-situ in a medium containing a pre-established Pt-ion concentration. The kinetics of growth involved Pt^{2+} ions even when the salt used for most of the experiments was $PtCl_4$. It was observed that the higher the Pt-ion concentration, the faster was the kinetics of degradation, which is to be expected. In PEMFC, some Pt-ion concentration exists at the two electrodes (in the presence of the ionomer and water). All those factors which tend to increase Pt-ion concentration will increase the kinetics of catalyst coarsening. At the cathode where oxidizing conditions exist, a higher Pt-ion concentration is expected, consistent with higher observed degradation. Thus, efforts should be devoted to designing catalyst/environment which tend to lower the Pt-ion concentration.

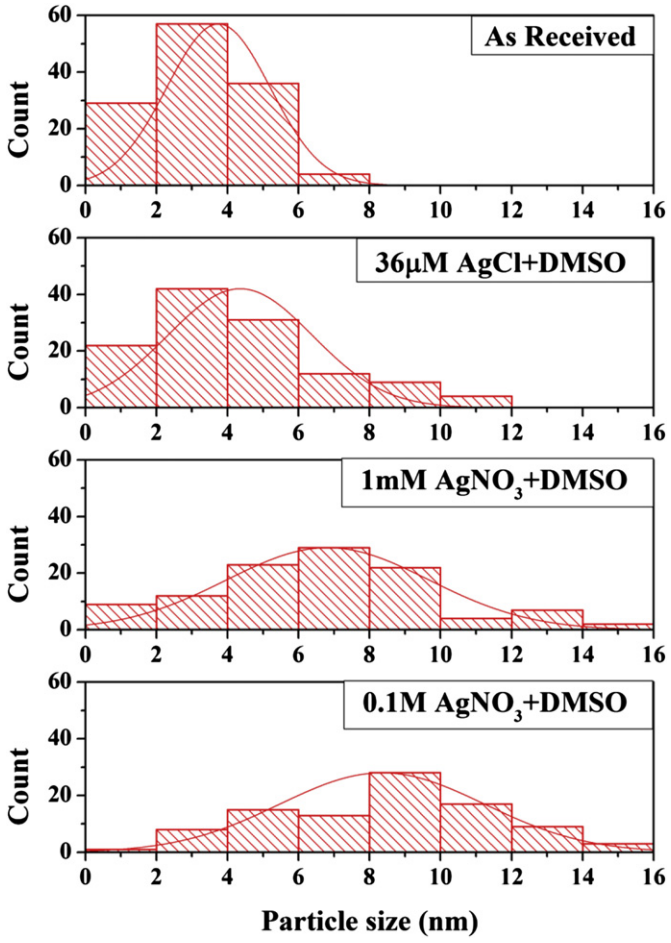

Fig. 12. Particle size distributions of n-Ag-catalyst supported on HAS carbon (BASF) treated in electrolyte solutions with various Ag^+ ion concentrations for 600 s using the experimental setup shown in Fig. 2.

4. Conclusions

The main objective of the present work was to investigate electrochemical Ostwald ripening/coarsening in platinum and silver commercial catalysts supported on high surface area (HAS) carbon. Ostwald ripening/coarsening was studied using an electrochemical method developed in this study. The procedure consisted of immersing two graphite rods: one with nano Pt or Ag painted on it and the other with bulk Pt or Ag wire wrapped around it in the corresponding electrolyte solution in DMSO. It was observed that nano Pt or Ag exhibited negative potential with respect to bulk Pt or Ag. This is consistent with the higher chemical potential of nano Pt or Ag compared to that of the bulk Pt or Ag due to the pressure created by the size (Gibbs–Thompson) effect. After the establishment of quasi-equilibrium, the voltage between the nano and the bulk electrodes decreased with increasing time as the nanoparticles coarsened. The coarsening process involves a coupled transport of Pt or Ag ions through the corresponding electrolyte and electrons through the carbon support/graphite rod. After 7 days in 0.1 M $PtCl_4$ + DMSO, nano Pt coarsened from 2.1 nm to 11.3 nm whereas nano Ag coarsened from 3.9 nm to 8.7 nm within just 10 min when treated in 0.1 M $AgNO_3$ + DMSO.

The effect of ion concentration in the coarsening kinetics of Pt or Ag was studied by treating samples in electrolytes with different concentrations of the dissolved salt. Both Pt and Ag exhibited faster kinetics when treated in electrolytes containing higher salt concentrations. The effect of the valence of the Pt ion (+2 vs. +4) on nano particle coarsening was studied by using $PtCl_2$ + DMSO and $PtCl_4$ + DMSO solutions of the same concentrations, 0.01 M. Coarsening of the Pt catalyst was faster when treated in 0.01 M $PtCl_2$ + DMSO solution as compared to that treated in 0.01 M $PtCl_4$ + DMSO. Despite high Pt^{4+} concentration in $PtCl_4$ + DMSO, the coarsening of Pt was slower due probably to lower Pt^{2+} concentration in the electrolyte containing $PtCl_4$. The present work suggests that efforts should be directed toward designing a PEMFC electrode environment which tends to lower the Pt^{2+} ion concentration, thus increasing catalyst stability.

Acknowledgments

This work was supported in part by the National Science Foundation under Grant Number CBET-0931080, the US Department of Energy under Grant Number DE-FG02-06ER46086, and the US Department of Energy EFRC Grant Number SC0001061 as a flow-through from the University of South Carolina.

References

[1] Y. Xu, A.V. Ruban, M. Mavrikakis, J. Am. Chem. Soc. 126 (14) (2004) 4717.
[2] R. Srivastava, P. Mani, N. Hanh, P. Strasser, Angew. Chem. Int. Ed. 46 (47) (2007) 8988.
[3] T. Toda, H. Igarashi, M. Watanabe, J. Electroanal. Chem. 460 (12) (1999) 258.
[4] S. Mukerjee, S. Srinivasan, M.P. Soriaga, J. McBreen, J. Electrochem. Soc. 142 (5) (1995) 1409.
[5] K. Kinoshita, Electrochemical Oxygen Technology, Wiley, New York, 1992, pp. 133–140.
[6] V. Jalan, E.J. Taylor, J. Electrochem. Soc. 130 (11) (1983) 2299.
[7] U. Koponen, H. Kumpulainen, M. Bergelin, J. Keskinen, T. Peltonen, M. Valkianen, M. Wasberg, J. Power Sources 118 (1–2) (2003) 325.
[8] B. Gurau, R. Viswanathan, R. Liu, T.J. Lafrenz, K.L. Ley, E.S. Smotkin, E. Reddington, A. Sapienza, B.C. Chan, T.E. Mallouk, S. Sarangpani, J. Phys. Chem. B. 102 (49) (1998) 9997.
[9] M.S. Wilson, F.H. Garzon, K.E. Sickhaus, S. Gottesfeld, J. Electrochem. Soc. 140 (10) (1993) 2872.
[10] R. Ornelas, A. Stassi, E. Modica, A.S. Arico, V. Antonucci, ECS Trans. 3 (1) (2006) 633.

[11] X. Wang, R. Kumar, D. Meyers, J. Electrochem. Solid State Lett. 9 (5) (2006) A225.
[12] J. Xie, D.L. Wood III, K.L. More, P. Atanassov, R.L. Borup, J. Electrochem. Soc. 152 (5) (2005) A1011.
[13] P.J. Ferreira, G.J. Lao, Y. Shao-Horn, D. Morgan, R. Makharia, S. Kocha, H.A. Gasteiger, J. Electrochem. Soc. 152 (11) (2005) A2256.
[14] W. Bi, G.E. Gray, T.F. Fuller, Electrochem. Solid State Lett. 10 (5) (2007) B101.
[15] K. Yasuda, A. Taniguchi, T. Akita, Z. Siroma, Phys. Chem. Chem. Phys. 8 (2006) 746.
[16] A. Ohma, S. Suga, S. Yamamoto, K. Shinohara, in: T. Fuller, et al. (Eds.), ECS Transactions, Vol. 3, 2006, pp. 519–529. No. 1.
[17] H. Liu, J. Zhang, F.D. Coms, W. Gu, B. Litteer, H.A. Gasteiger, in: T. Fuller, et al. (Eds.), ECS Transactions, Vol. 3, 2006, pp. 493–505. No. 1.
[18] A. Laconti, H. Liu, C. Mittelsteadt, R. McDonald, in: T. Jarvi, et al. (Eds.), ECS Transactions, Vol. 1, 2005, pp. 199–219 (8).
[19] B. Merzougui, S. Swathirajan, J. Electrochem. Soc. 153 (12) (2006) A2220.
[20] K.L. More, R. Borup, K.S. Reeves, ECS Trans. 3 (1) (2006) 717.
[21] A.V. Virkar, Y. Zhou, J. Electrochem. Soc. 154 (6) (2007) B540.
[22] C. Yu, E.F. Holby, R. Yang, M.F. Toney, D. Morgan, P. Strasser, ChemCatChem 4 (6) (2012) 766.
[23] O.F. Devereux, Topics in Metallurgical Thermodynamics, John Wiley-Interscience, New York, 1983.
[24] J.B. Eberhart, S. Horner, J. Chem. Educ. 87 (2010) 608.
[25] L. Vitos, A.V. Ruban, H.L. Skriver, J. Kollár, Surf. Sci. 411 (1998) 186.
[26] I.M. Lifshitz, V.V. Slyozov, Phys. Chem. Solids 19 (1961) 35.
[27] C. Wagner, Z. Elektrochem. 65 (1961) 581.
[28] P. Parthasarathy, A.V. Virkar, J. Electrochem. Soc. 157 (2010) B768.
[29] P. Parthasarathy, A.V. Virkar, J. Power Sources 196 (2011) 9204.
[30] R.G. Linford, in: M. Green (Ed.), Solid State Surface Science, Marcel Dekker, New York, 1973.